



Organic solar powered greenhouse performance optimization and global economic opportunity

Journal:	<i>Energy & Environmental Science</i>
Manuscript ID	EE-ART-11-2021-003474.R2
Article Type:	Paper
Date Submitted by the Author:	09-Mar-2022
Complete List of Authors:	Ravishankar, Eshwar; North Carolina State University, Mechanical And Aerospace Engineering Booth, Ronald; North Carolina State University, Mechanical and Aerospace Engineering Hollinsworth, Joseph; North Carolina State University, Civil, Construction, and Environmental Engineering Ade, Harald; North Carolina State University, Physics Sederoff, Heike; North Carolina State University, Plant and Microbial Biology DeCarolis, Joseph; North Carolina State University, Civil, Construction, and Environmental Engineering O'Connor, B.; North Carolina State University, Mechanical and Aerospace Engineering

Organic solar powered greenhouse performance optimization and global economic opportunity‡

Eshwar Ravishankar,^a Ronald E. Booth,^a Joseph A. Hollinsworth,^b Harald Ade,^c Heike Sederoff,^d
Joseph DeCarolis^b and Brendan T. O'Connor^{a*}

^a Department of Mechanical and Aerospace Engineering, and Organic and Carbon Electronics Laboratories (ORaCEL), NC State University, Raleigh, NC, 27695, USA.

^b Department of Civil, Construction, and Environmental Engineering, NC State University, Raleigh, NC, 27607, USA.

^c Department of Physics, and ORaCEL, NC State University, Raleigh, NC, 27695, USA.

^d Department of Plant and Microbial Biology, NC State University, Raleigh, NC, 27607, USA.

*Correspondence and Lead Contact: btoconno@ncsu.edu

‡ Electronic supplementary information (ESI) available: []. See DOI:

Abstract: Greenhouses conserve land and water while increasing crop production, making them an attractive system for low environmental impact agriculture. Yet, to achieve this goal, there is a need to reduce their large energy demand. Employing semitransparent organic solar cells (OSCs) on greenhouse structures provide an opportunity to offset the greenhouse energy needs while maintaining the lighting needs of the plants. However, the design trade-off involved in optimizing solar power generation and crop productivity to maximize greenhouse economic value is yet to be studied in detail. Here, a functional plant growth model is integrated with a dynamic energy model that includes supplemental lighting to optimize the economics of growing lettuce and tomato. The greenhouse optimization considers 64 different OSC active layers with varying roof coverage for 25 distinct climates providing a global perspective. We find that crop yield is the primary economic driver, and that crop yield can be maintained in OSC-greenhouses across diverse climates. The crop productivity along with the energy produced by the OSCs results in improved net present value of the OSC-greenhouses relative to conventional systems in most climates for both lettuce and tomato. In addition, we find common solar cell active layers that maximize greenhouse economic value resulting in guidelines for scaling up OSC-greenhouse design. Through this model framework, we highlight the opportunity for OSCs in greenhouses, uncover designs and locations that provide the most value, and provide a basis for further development of OSC-greenhouses to achieve a sustainable means of food production.

1 Introduction

Agriculture has far sweeping impacts on the environment that include ecosystem degradation, freshwater stress, biodiversity loss, and is a large contributor to greenhouse gas emissions. For example food systems are responsible for a third of global anthropogenic greenhouse gas emissions, in which land-use and land-use change were a major contributing factor.¹ One approach to alleviate agriculture's environmental impact is through controlled environmental food production, and in particular greenhouses. Greenhouse agriculture is an intensive food production approach that can significantly reduce agricultural land use, while also being productive across diverse climates. In addition, greenhouses can operate year around, significantly reduce water consumption, and offer protection against extreme weather events. However, greenhouses can be energy intensive relative to conventional farming.^{2,3} This energy consumption is largely related to controlling the greenhouse climate and the use of supplemental lighting. For greenhouses to contribute to a more ecologically responsible agri-food industry there is a need for them to reduce external energy demand. Incorporating solar power onto greenhouse structures has recently attracted attention as an approach to minimize, or even completely eliminate greenhouse external energy demand.⁴ Semitransparent organic solar cells (ST-OSCs) are particularly promising for greenhouse integration with attributes that include spectrally tunable transparency,⁵ and compatibility with thin flexible form factors for simple module integration.^{6,7,8} OSCs have also been making significant strides in power conversion efficiency, which now approach 20 %.^{6,9} These improvements in efficiency have largely been due to the arrival of non-fullerene electron acceptors with complimentary absorption to that of high-performance polymer donors.¹⁰ At the same time, non-fullerene acceptors can shift light absorption into the near infrared thereby reducing absorption overlap with the photosynthetically active radiation (PAR) spectrum (400 nm – 700 nm) essential to plant growth.^{11–18} Finally, recent demonstrations of large-area non-fullerene based OSCs are improving the commercial outlook of the technology.¹⁹

The potential of OSC-integrated greenhouses has been highlighted through several studies that focus on the impact of semitransparent OSCs on plant growth. This includes demonstration of the growth of mung bean sprouts, pepper, tomatoes, lettuce, and medicinal plants under functional ST-OSCs or mock OSC-filters.^{15,20–23} While some studies were for only short durations, many of the longer duration studies showed promising plant performance. Pepper and lettuce showed plant growth with minimal impact on crop yield.^{20,21} Tomatoes grown under ST-OSC occupying nearly

50 % of the total greenhouse roof area showed a 10 % drop in yield with respect to the control.²³ However, during the period where the control experiments were shaded in the summer, tomatoes grown under the ST-OSC had comparable yield. In addition to plant productivity, we recently reported an analysis of the energy demand of OSC-greenhouses for diverse climate locations across the United States.²⁴ We demonstrated that net zero energy (NZE) greenhouse systems can be realized in warm and moderate climates with the addition of moderately efficient ST-OSCs of the order of 10 %.²⁴ While these studies show tremendous promise for OSC-integrated greenhouses, they have focused solely on plant growth under OSCs,^{15,20–23} or have looked at energy demand in OSC-greenhouses.²⁴ There remains a need to consider the system holistically, considering the trade-offs in energy demand and crop productivity to maximize economic value.

Modeling plant growth under OSCs provides a means to estimate plant yield along with greenhouse energy demand and OSC power generation, guiding ST-OSC design. Previously, to account for plant productivity under OSCs, a crop growth factor (CGF) was introduced which assumed plant growth is linearly proportional to the incident solar radiation over the PAR spectrum.⁵ While the CGF provides a path to quantify the trade-off between crop productivity and power generation, the model is oversimplified. For example, the linear dependence of crop production with illumination is not applicable for low-light requiring crops such as lettuce, spinach and basil.^{21,25} In addition, the model does not take into account greenhouse operating practices such as the use of shade-cloths, or the impact of other greenhouse environmental factors such as temperature.²⁶ Here, we perform an OSC-greenhouse optimization with the economic value being the figure of merit that includes a detailed accounting of lighting, energy demand, greenhouse climate, and plant productivity, as illustrated in **Figure 1**. We combine our previous work on energy balance of OSC-greenhouses,²⁴ with a functional plant growth model. The plant model accounts for plant specific lighting needs including intensity and spectra, local greenhouse temperature, and carbon dioxide.^{27,28} The system optimization considers 64 unique OSC active layers in combination with varying greenhouse roof area coverage. The plants considered are lettuce (cv. berlo²⁷) and tomato (cv. trust variety²⁸), which are chosen as they are popular greenhouse crops, and represent a low-light tolerant and high-light requiring crop.^{29,30} Given the high light demands of tomato, supplemental lighting through LED light sources is considered in the system optimization for tomato production. The model is then applied to greenhouses in 25 locations across the globe that have distinct climates following the Köppen-Geiger classification

system.³¹ For each location, the net present value (NPV) of the OSC-greenhouse is determined relative to a conventional greenhouse. While popular greenhouse crops will vary with location, lettuce and tomato provide model systems that span the lighting demands of a broad range of popular greenhouse crops, as listed in **Table S1**. Through this optimization, we find that OSC-greenhouses growing lettuce can achieve NZE with a minimal drop in yield in 11 of the 25 climates considered. Similarly, we find potential for achieving NZE in 10 climates when growing tomatoes. In most of the other climates, crop production could be largely maintained while the OSCs contribute to the majority of the greenhouse energy needs. Overall, there was an increase in NPV in the OSC-greenhouses in comparison to a conventional greenhouse for both lettuce and tomato in all but 9 climates. The maximum NPV was found to be 870 \$/m² for lettuce and 610 \$/m² for tomato, given on a per unit greenhouse floor area. A maximum gain in NPV of \$305/m² and \$390/m² was seen for lettuce and tomato production respectively for ST-OSC greenhouses across various climates. These gains are substantial relatively to the NPV range obtained for the conventional system, which includes cases where the economic outlook shifts from a negative NPV for a conventional system to a positive NPV with the addition of OSCs. These results provide support that ST-OSC integration will improve the economic potential of greenhouses while significantly offsetting their energy demand, providing an opportunity for high intensity low environment footprint agriculture.

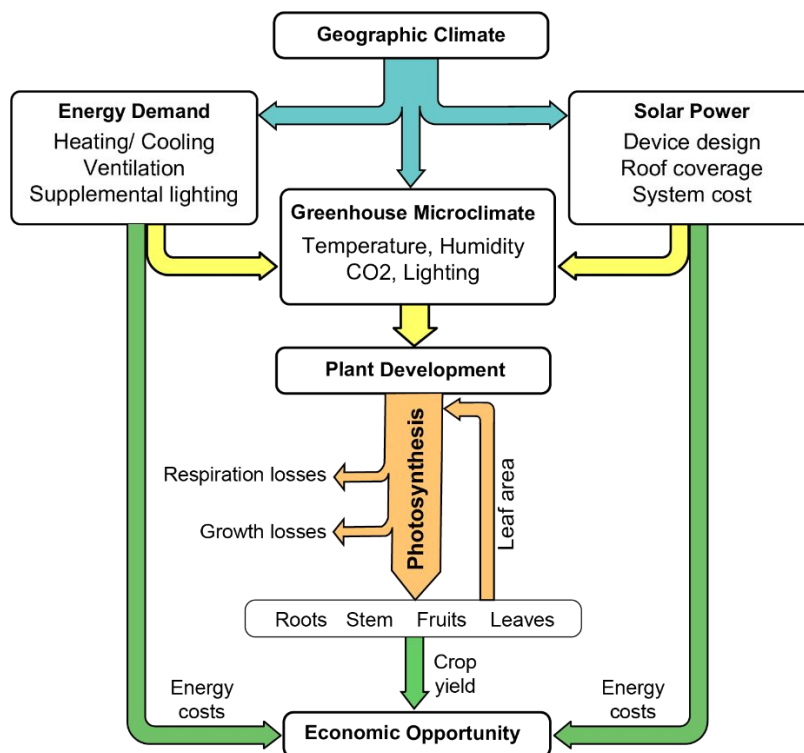


Figure 1. Flowchart relating greenhouse economics (in the form of NPV) to net plant yield, energy demand and solar energy generation from integrated semitransparent organic solar cells. The complete greenhouse performance is characterized based on climate.

2 Methods

2.1 Plant Growth Model

A brief overview of the processes involved in modelling the growth of lettuce and tomato is provided here with additional details provided in the **supporting information**. The daily light integral (DLI) is the photon flux in the PAR spectrum received over the entire day. While lettuce has an optimal DLI of around 13-17 moles m⁻² day⁻¹, tomato often requires a higher DLI of 22 - 30 moles m⁻² day⁻¹ typically met through the use of supplemental lighting.³⁰ The functional plant growth model tracks the rate of change of dry matter of the selected crop, which can include leaves, stem, root, flowers, and fruit (as appropriate for the plant). The dry matter addition considers the rate of photosynthesis and plant leaf area while accounting for associated biological losses. The rate of photosynthesis in turn is determined by the greenhouse environmental conditions including light, temperature, humidity, and CO₂.³² Supplemental lighting was included in the tomato

modeling to meet the minimum DLI requirements as needed for various stages of the plant development from germination to flowering and fruit harvest,³³ as provided in **Table S7**. The impact of light spectrum on plant growth was included for lettuce and validated with experimental results, as shown in **Figure S2**.²¹ The model assumes that there is sufficient spacing between plants to ensure no self-shading caused by overlap in leaves. Light spectrum was not considered for tomato due to the strong cultivar dependence and the inability to validate the results.³⁴ For lettuce, the rate of photosynthesis is dependent on the ratio of light intensity in the red (600-700 nm) and blue (400-500 nm) (R:B) wavelength range incident on the plant as given in **Figure S2(A)**.³⁵ R:B ratio also influences the change in leaf area and fractional biomass partition to root and shoot. In addition to carbon fixation, plants experience loss in assimilated carbon content due to respiration and growth-related losses.^{32,36} The rate of losses in lettuce is influenced by the fraction of biomass partitioned to root and shoot which is shown in **Figure S2(B)**. Leaf area of the plant increases as a fraction of the available biomass generated.³⁷ The fraction is determined by a parameter called specific leaf area (SLA). The SLA is influenced by both light intensity and % blue (400-500 nm) light over the PAR spectrum, as shown in **Figure S2(C)**.³⁷ Finally, we assess total yield based on the harvested dry mass. The dry mass was partitioned into various components of the plant including root, stem and in case of tomato - flowers and fruit. Input parameters for modelling lettuce and tomato are provided in **Table S2** and **Table S3** respectively. The model results were validated by comparing to experimental studies and other models as shown in **Figure S3**.^{21,27,28} The plant model assumes that plant growth is not impacted by factors such as genetics or epigenetics. For lettuce, the parameters used in the plant model were calibrated using averaged experimental data for lettuce growth measured under three different OSC filters across three different replications.²¹ This to a certain extent accounts for variability in plant growth as shown in **Figure S2**. However, for tomatoes experimental study under OSCs was not performed and hence we directly adapt the parameters provided in literature which does not account for any variability.²⁸

2.2 OSC Performance Modeling

The solar cell structure utilized for modelling is shown in inset **Figure 2(A)** and consists of a 100 nm thick indium tin oxide (ITO) layer used for the front electrode followed by a 35 nm thick ZnO electron transport layer (ETL) and then the active layer. After the active layer, there is

a 5 nm MoO₃ hole transport layer (HTL) followed by another 100 nm thick ITO electrode. This solar cell structure is sandwiched between 2 mm thick layers of glass that acts as encapsulation. In considering the transmittance of the solar cells, the ITO, HTL and ETL reduce transmittance over the PAR spectrum uniformly. Thus, the bulk heterojunction (BHJ), or active layer comprising of a blend of organic semiconductors, plays the primary role in dictating the transmission spectrum of the OSC. The key parameters for the ST-OSCs are power conversion efficiency (PCE) and transmittance over PAR. These parameters compete with each other in the greenhouse system optimization. It is often considered ideal to have a ST-OSC with absorption spectra that is minimized over PAR spectrum to reduce impact on plant growth. In this case, materials that absorb light primarily in the IR may be preferred but this comes at the cost of losing open circuit voltage (V_{OC}) and potentially PCE. Thus, we consider 64 high performance OSC active layer blends comprised of electron donors and acceptors with unique spectral absorption characteristics, as shown in **Figure 2(B)** and **Figure 2(C)**. These active layer blends comprise of a broad array of polymer donors and small molecule acceptors (SMAs), a ternary and an all-polymer active layer system. The absorption spectra of materials have been categorized based on the long wavelength absorption edge, which varies from 700 – 1100 nm.

The transmittance, absorptance, and short circuit current through the ST-OSC stack were determined through a transfer matrix model.^{38,39} The modeled external quantum efficiency (EQE) was compared to the reported EQE of the OSCs to ensure accurate predictions of short circuit current. To estimate power generation, we use the reported V_{OC} at 1-sun illumination for the reference opaque device, which was then varied based on an equivalent circuit photodiode model using the modeled short circuit current.²⁴ The power generation corresponds to the maximum power point of the solar cells under all conditions.²⁴ The complete list of active layers with modelled OSC efficiency, transmittance and corresponding opaque device efficiency are given in **Table S4**. The OSCs were modelled with active layer thicknesses that correspond to the best performing reference opaque device. There is potential for further OSC optimization through varying the active layer thickness, and through the use of external optical coatings such as Bragg reflectors.^{21,24} We did not consider these OSC optimization schemes here and may further improve the modeled outlook. The fill factor of the cells was also taken from reference reports and were considered a constant. We observe a range in PCE from 5 % to just under 16 % while the transmittance varies from 20 % to nearly 60 %. The relationship between PCE and transmittance

over PAR for the solar cells considered is shown in **Figure 2(A)**. There is a linear trade-off between transmittance and PCE indicating the importance of mapping crop growth and OSC power generation to better establish this performance trade-off.

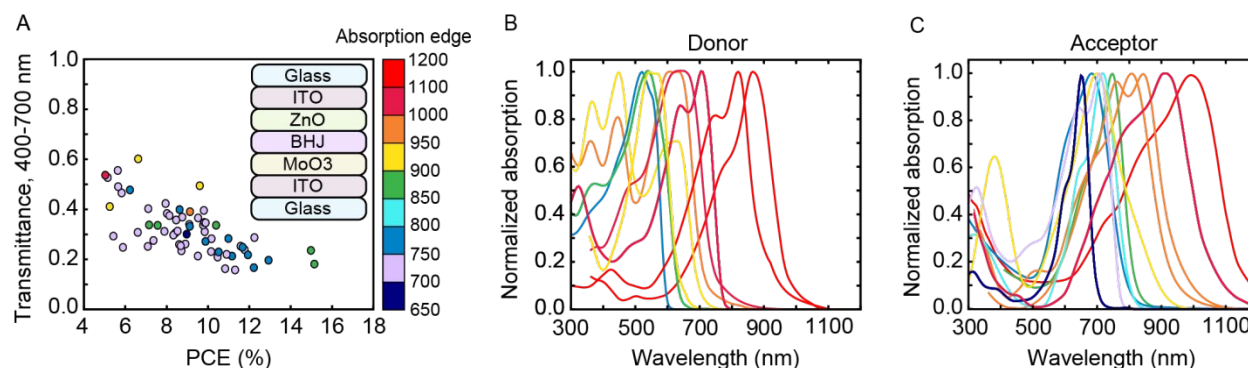


Figure 2. (A) Trade-off between transmittance over PAR and PCE; *inset*: device stack of modelled ST-OSC systems. Normalized absorption of select (B) donor and (C) acceptor organic semiconductors.

2.3 Climate Selection and Greenhouse Operation

To classify greenhouse energy demand and plant yield as a function of global climates, we utilize the Köppen-Geiger climate classification system.³¹ This system includes a total of 30 different climates categorized based on temperature patterns and precipitation. Here, we consider 25 of these climates by modeling a representative city for each climate with details provided in **Table S4**. The omitted 5 climates are rare and represent a negligible fraction of geographical land.⁴⁰ A detailed description of each climate category is provided in **Section 3** in the **supporting information**. In each location, a year-around operating greenhouse was simulated with the OSCs placed on the roof. Five solar module roof area coverages were considered that varied from 20 % - 100 %. A standard commercial single span gable-roof greenhouse of dimensions 29.4 x 7.3 m with a gutter height of 3 m was chosen for simulation across all the climates.⁴¹ The greenhouse is oriented north-south and a tilt angle of 27° is assumed for the east-west facing roof.⁴² The roof and walls excluding the north-facing wall were made up of 4 mm thick single pane glass. The north wall was considered an adiabatic surface, which is often the location of a head house or storage area. All other walls were modeled with solar and thermal transmission. A 25 % loss in transmittance of light entering the greenhouse was considered.⁴² Other specifications for

ventilation, heating and shading operation followed our previous reported work.²⁴ Shade cloths with 50 % transmittance were deployed based on standard operating practices to maintain greenhouse temperature. Details of the shade deployment schedule for both ST-OSC and reference greenhouses are provided in **Table S5**.

For modelling lettuce, the night temperature was set to 15-18 °C and the day temperature is set to 21-25 °C.⁴³ Relative humidity across the entire day was controlled to be between 60 - 80 %. A lettuce planting density of 18 plants/m² greenhouse floor area was assumed.³² Across the entire year, we consider multiple cycles of lettuce growth with the start of the cycle marked by the germination phase and the conclusion of the cycle demarcated by harvest. Here, we consider a harvest every month in the simulated greenhouse across all the considered climates.⁴³ For modelling tomato, the night temperature was set to 17-22 °C and day temperature was set to 24-30 °C. Relative humidity across was controlled to be between 60 %-80 %.³⁰ Two harvest cycles were considered for tomato production. In the first cycle, the plants were seeded around January and were harvested through June after fruit development begins. The second cycle started in July and were harvested through the end of year, again upon the onset of fruiting period. A planting density of 4 plants/m² greenhouse floor area was assumed.²⁸ Supplemental lighting was considered to be active from the onset of plant germination till fruit production. A 300 W LED lamp was modeled providing a photosynthetic photon flux density (PPFD) of 180 $\mu\text{moles m}^{-2} \text{s}^{-1}$ across a 10 x 10 ft² area.⁴⁴ Prior to the onset of flowering (determined by the number of nodes or side stems formed), supplemental lighting was turned on to ensure minimum DLI does not fall under 7 moles m⁻² day⁻¹. From the flowering stage, supplemental lighting was turned on to ensure a minimum DLI of 22 moles m⁻² day⁻¹.³⁰ A maximum lighting duration of 20 hours was imposed.⁴⁵ The LEDs utilized for supplemental lighting was assumed to have a conversion rate from electrical input to PAR output of approximately 60 % with a spectrum that matches sunlight. The remaining 40 % of electrical input was converted to heat inside the greenhouse space.⁴⁶ The climate parameters for each location were taken on an hourly basis from Typical meteorological year 3 (TMY3) data set.⁴⁷ The monthly average beam and total solar radiation data incident on a horizontal surface were obtained from national solar database (NSRDB)⁴⁸ which is then utilized to determine the hourly direct, diffuse, and reflected solar radiation on the greenhouse walls and roof.⁴⁹ All simulations were conducted in MATLAB, and executed on a high-performance computing system cluster, which included over 16,000 simulations. The high-performance computing is not a mandatory

requirement for running the program. However, considering the extent of case scenarios computed in this work, we employed parallel computing to conserve time through the NCSU Henry2 Linux high performance computing cluster. Each simulation was completed on a pair of eight core Intel Xeon processor and took approximately 200 minutes to complete.

2.4 Economic Framework

To assess the economic opportunity of the OSC-greenhouses the NPV of the system was determined considering system capital costs, operating costs including energy costs, and crop revenue. The NPV used a discount rate of 10 % assuming a greenhouse lifetime of 30 years. The cost of OSCs include cost of material, fabrication, degradation rate, labor, taxes, depreciation, and balance of system equipment.^{51,52} Three sets of OSC cost parameters termed “base case”, “optimistic” and “conservative” values were used to determine the impact on NPV. The base case parameters considered an OSC lifetime of 10 years, with a geometric fill factor of 85 %.^{24,50} The optimistic parameters represent aspirational performance and considered an OSC lifetime of 20 years, with a geometric fill factor of 90 %. On the other hand, the conservative values consider the maximum possible cost for OSC manufacturing, and balance of system equipment. An OSC lifetime of 5 years was considered and a geometric fill factor of 80 % was assumed. Furthermore, a 25 % loss in performance due to device scale-up was factored in. The inputs for computing LCOE for all three cases are provided in **Table S6**. Across all three cases, the present cost of the OSCs over the period of the greenhouse lifetime was normalized with respect to the corresponding solar power generated to create a levelized cost of energy (LCOE). Given that a 30-year greenhouse lifetime is considered, the analysis includes replacement of the OSCs at the end of their lifetime. The value of the modules to be replaced were assumed to be priced at a value that is half of its original manufacturing cost.⁴⁸ The LCOE was then used to compute cost of generating solar energy for offsetting greenhouse energy demand. The LCOE for each selected climate is provided in **Table S5**. Revenue streams are inclusive of annual income, annualized cost of loan payments associated with capital costs, and annual variable cost that comprised of heating, cooling, and supplemental lighting. When annual greenhouse energy demand exceeded solar energy generated, the energy deficit was assumed to be offset by energy from the grid. While net metering was employed on an annual basis, there is no assumed economic value included for an annual surplus of electricity generation.⁵¹ For conventional greenhouses, the complete greenhouse energy demand

was assumed to come from the grid. To simplify calculations, the crop revenue was based on \$/kg, net metering was considered for electricity consumption and generation, and capital costs were assumed to be constant independent of location. The annualized investment cost includes the cost of the OSCs and greenhouse structure, each calculated using a capital recovery factor which gives a measure of the annual payment on a capital investment. Fertilizer, water, and labor costs were assumed to be constant across all considered locations and for the greenhouse lifetime. Inputs for greenhouse costs and revenue is shown in **Table S5**. Importantly, many of the costs of the system will be location-specific. Establishing specific economic analysis for each geographic location is beyond the scope of this work. Here, we use costs that are commensurate with expected costs for systems installed in the United States, and focus specifically on NPV differences between an OSC-greenhouse and a conventional greenhouse. This approach is expected to provide a reasonable outlook on the relative opportunity to install OSCs on a greenhouse system.

3 Results and Discussion

We report here the “base case” annual performance of the OSC-greenhouses with a focus on nine distinct climates selected from the above mentioned 25 climates that highlight the role of climate on the design optimization and system performance. The base case OSC-greenhouse optimization results for growing lettuce and tomato for the remaining 16 climates are provided in **Figure S5-S8** and **Figure S9-S12**. Results of the optimistic and conservative NPV in comparison to the base case NPV of the OSC-greenhouses for lettuce and tomato is provided in **Figure S13**. Below, we first consider system performance when growing lettuce, then consider tomato.

3.1 OSC-Greenhouse Optimization for Lettuce

The annual OSC-greenhouse performance metrics including net greenhouse energy demand, lettuce yield, and NPV gain with respect to conventional greenhouses for the different OSC configurations is given in **Figure 3**. The yield is provided relative to the conventional greenhouse and the energy demand is reported against the total solar power generation. We find that crop yield is the primary economic driver, and that OSC systems that reduce yield loss while providing substantial energy offset relative to a conventional greenhouse have the best economic potential. While yield drives the economic potential, the addition of the OSCs resulted in the ability

to achieve NZE greenhouses in seven of the nine climates, as shown in **Figure 3**. However, there is a clear trade-off in energy demand and annual lettuce production, which is climate specific.

Climates with latitudes lower than 35° (tropical, hot and temperate highland) are warm year around, and thus have a relatively low energy demand of under $150 \text{ kWh/m}^2\text{-year}$ associated mainly with cooling. In these climates, there is a broad range of OSC systems that result in crop yield that is similar or better than the conventional system while the solar cells completely meet the greenhouse energy needs, as shown in **Figure 3(A-C)**. The addition of the OSCs resulted in an improvement in lettuce yield of up to $4.5 \text{ kg/m}^2\text{-year}$ for the tropical savanna climate. This improvement in yield over the conventional systems is attributed to improved thermal management of the greenhouse space as discussed below in **section 3.3**. The OSC cells that maximize NPV in the warmer climates were found to consist of either DPP2T:IEICO-4F (absorption edge of 950 nm) or D18:Y6 (absorption edge of 910 nm) active layers. The DPP2T:IEICO-4F OSC has a PCE of 6 % and PAR transmittance of 60 %. Optimized performance was achieved with 80 % -100 % roof area coverage. The D18:Y6 has a PCE of 15 % and transmittance of only 20 %. The lower transmittance of the cells requires a lower roof coverage fraction (20 % - 40 %) to ensure crop production is maintained. Optimizing for NPV, these climates provide a maximum NPV of up to $\$705/\text{m}^2$ of greenhouse floor area, which amounts to a gain in NPV of $\$310/\text{m}^2$ in comparison to conventional greenhouses, nearly doubling the greenhouse economic potential.

At latitudes between 35° to 40° , hot summer mediterranean (temperate and snow) climates have lower solar insolation and the greenhouses experience up to a $2 \text{ kg/m}^2\text{-year}$ drop in annual lettuce yield when achieving net zero energy (**Figure 3(E-F)**). However, the temperate highland climate (**Figure 3(D)**) shows potential to achieve net zero energy greenhouses while also improving annual lettuce yield by $1 \text{ kg/m}^2\text{-year}$. Alternatively, OSC-greenhouses in these climates can be designed to maintain crop yield while meeting over half of the annual energy demand of the greenhouse. Given the large impact of yield on economic outlook, minimizing yield loss resulted in the greatest gains in NPV. Furthermore, these climates are more conducive to maintaining the greenhouse set-point temperature year around leading to higher lettuce yield than tropical or hot climates. Hence a higher nominal NPV is seen in these climates for conventional greenhouses. The OSCs that maximize NPV in these climate consisted of PTB7-TH:IEICO-4F (absorption edge of 950 nm) active layer with 60 % roof coverage and a D18:Y6 active layer with 40 % coverage. The OSC with PTB7-TH:IEICO-4F active layer had a PCE of 11 % and PAR

transmittance of 43 %. The higher transmittance of this OSC allowed for greater roof coverage without crop loss. These climates provide a maximum NPV of up to \$780/m² of greenhouse floor area for the OSC-greenhouses, which equates to an increase of \$85/m² in NPV in comparison to the conventional greenhouses.

Finally, temperate climates composed of oceanic and subarctic climates as well as snow and tundra climates at latitudes higher than 40° have prolonged winter combined with low insolation resulting in higher energy demand from 250 kWh/m²-year to 500 kWh/m²-year, as shown in **Figure 3(G)-(I)**. The low insolation results in a very low tolerance to utilize solar energy from OSCs without impacting plant growth. This is depicted by the variation in annual lettuce yield as a function of average annual DLI in snow climate in **Figure S4(B)**. The model shows that 20 % - 40 % ST-OSC roof area coverage of DPP2T:IEICO-4F is possible to offset partial energy demand without yield loss. These systems showed little benefit from both an economic and energy offset perspective in comparison to a conventional greenhouse. The OSC-greenhouses in these climates provide a maximum NPV of about \$675/m² equating to a marginal gain in NPV of less than \$10/m² in compared to a conventional greenhouse.

In comparison to the base case scenario, the change in NPV for the optimistic case considering a 20-year OSC lifetime and 90 % geometric fill factor was observed to be negligible as shown in **Figure S13(A)**. This is attributed to the annual plant yield having a significant impact on NPV and the preference for low roof area coverage of OSCs in multiple climates for lettuce growth. However, for the conservative values, factoring for a lower geometric fill factor, manufacturing and operation costs as well as efficiency loss from scale-up, we observe a significant drop in NPV (**Figure S13(A)**).

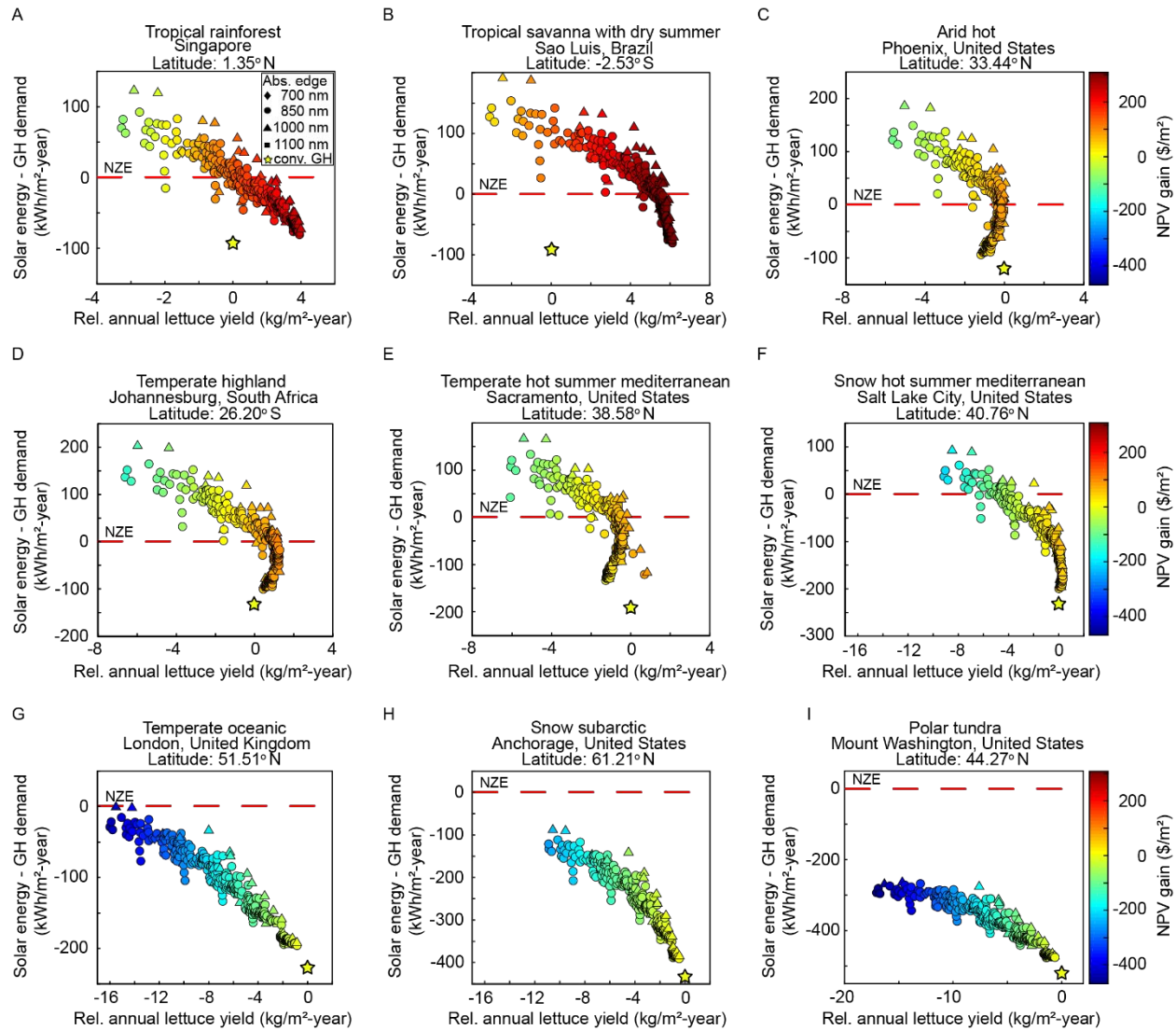


Figure 3. The relative gain in base case NPV per unit greenhouse floor area when adding OSCs as a function of relative annual lettuce yield and difference between solar energy and greenhouse demand across nine distinct climates. The data includes modeling 64 OSC active layers organized by the cells absorption edge. The specific location modeled for a given climate classification is listed above the plots. Lettuce yield and NPV gain is measured relative to the conventional greenhouse system for each climate. The performance of the conventional system is given by a star symbol for each climate.

3.2 OSC-Greenhouse Optimization for Tomato

The OSC-greenhouse optimization for tomato was considered for the same nine climates selected for lettuce, with the results given **Figure 4**. The results for the remaining 16 climates are

provided in **Figure S9-S12**. In contrast to growing lettuce, we consider supplemental lighting for tomato production to ensure the DLI does not fall below a desired set point over the plant's growth. The target DLI over this growth cycle is given in **Table S7**. With the addition of supplemental lighting, greenhouse energy demand for the conventional greenhouses ranges from 220 kWh/m²-year to about 620 kWh/m²-year when operating in climates ranging from tropical to tundra. Overall supplemental lighting adds 15 % - 50 % to the annual greenhouse energy demand compared to lettuce production.⁵³ At the same time, supplemental lighting helps minimize differences in the DLI incident on the tomatoes when considering the different OSCs. However, since the supplemental lighting ensures only that a minimum DLI was provided, this does not result in the same DLI between the conventional and OSC greenhouses. The differences in hourly solar insolation continue which also results in differences in greenhouse temperature. These temperature changes result in moderate differences in the annual yield across the different OSC systems considered.

Across the tropical and dry climate at latitudes lower than 35° we find net zero energy greenhouses with a maximum gain in fruit yield of 2 kg/m²-year with respect to the conventional greenhouse, as shown in **Figure 4(A)-(C)**. These climates provide a maximum NPV of up to \$300/m² of greenhouse floor area, which is an increase of approximately \$320/m² of greenhouse floor area in comparison to conventional greenhouses. The low NPV of conventional greenhouses in these climates is attributed to additional energy demand caused by supplemental lighting. Furthermore, in the absence of significant drop in light due to supplemental lighting, greenhouses in tropical and dry climates suffer from insufficient heat regulation in the summer even after shading leading to reduced fruit yield in comparison to greenhouses operating in cooler climates. This causes a negative revenue stream and hence a negative NPV. Better IR sunlight management in OSC-greenhouses leads to improved yield and coupled with energy offset results in significant gain in NPV.

Locations at latitudes between 35° to 40° can achieve near to complete energy neutrality with a minor drop in annual tomato fruit yield of 1 kg/m²-year relative to the conventional greenhouse, as shown in **Figure 4(D)-(F)**. Alternatively, optimizing for maximum NPV, the OSC-greenhouses can largely maintain tomato yield while meeting a large fraction of the greenhouse energy needs resulting in a maximum NPV of around \$290/m² of greenhouse floor area providing a gain in NPV of about \$75/m² in comparison to conventional greenhouses. At higher latitudes

above 40°, temperate oceanic and subarctic climates as well as snow and tundra climates have high energy demand and hence the OSCs only partially offset greenhouse energy demand with a maximum drop in fruit yield of 1 kg/m²-year relative to the conventional greenhouse as shown in **Figure 4(G)-(I)**. Contrary to lettuce growth at comparable climates, the minimal change in annual fruit yield coupled with a 20 % - 65 % offset in greenhouse energy demand, results in substantial gains in NPV with respect to the conventional greenhouse. A maximum NPV of about \$610/m² is seen for these climates, which amounts to a gain in NPV of about \$390/m² with respect to conventional greenhouses.

All nine climates had a 60 % - 100 % OSC roof area coverage of PM6:Y6 based OSCs to maximum energy offset. The OSC stack with PM6:Y6 as the active layer has the lowest PAR transmittance among the selected active layers at 20 % and has the highest PCE at 15 %. While the transmittance is low, there remains significant lighting that enters through the walls of the greenhouse particularly in the winter, as previously discussed.²⁴ A 100 % OSC roof area coverage of PM6:Y6 OSC stack increases the supplemental lighting energy need by an average of only about 45 kWh/m²-year across the considered climates. This is more than offset by the energy generated from the ST-OSC. Through better temperature control provided by the OSCs, improvement in annual tomato fruit yield was found across tropical and dry climates as shown in **Figure 4(A)-(C)** and temperate mediterranean climate as shown in **Figure 4(E)**.

Similar to lettuce, the change in NPV for the optimistic case for tomato was observed to be negligible as shown in **Figure S13(B)**. This is once again attributed to the annual plant yield having a significant impact on NPV. While the conservative values once again demonstrate significant drop in NPV compared to base case and optimistic values, we observe that the effect is less pronounced for tomatoes. This is attributed to a preference for higher OSC roof area coverage as well as a higher efficiency device due to the need to power supplemental lights in addition to heating and ventilation energy demand.

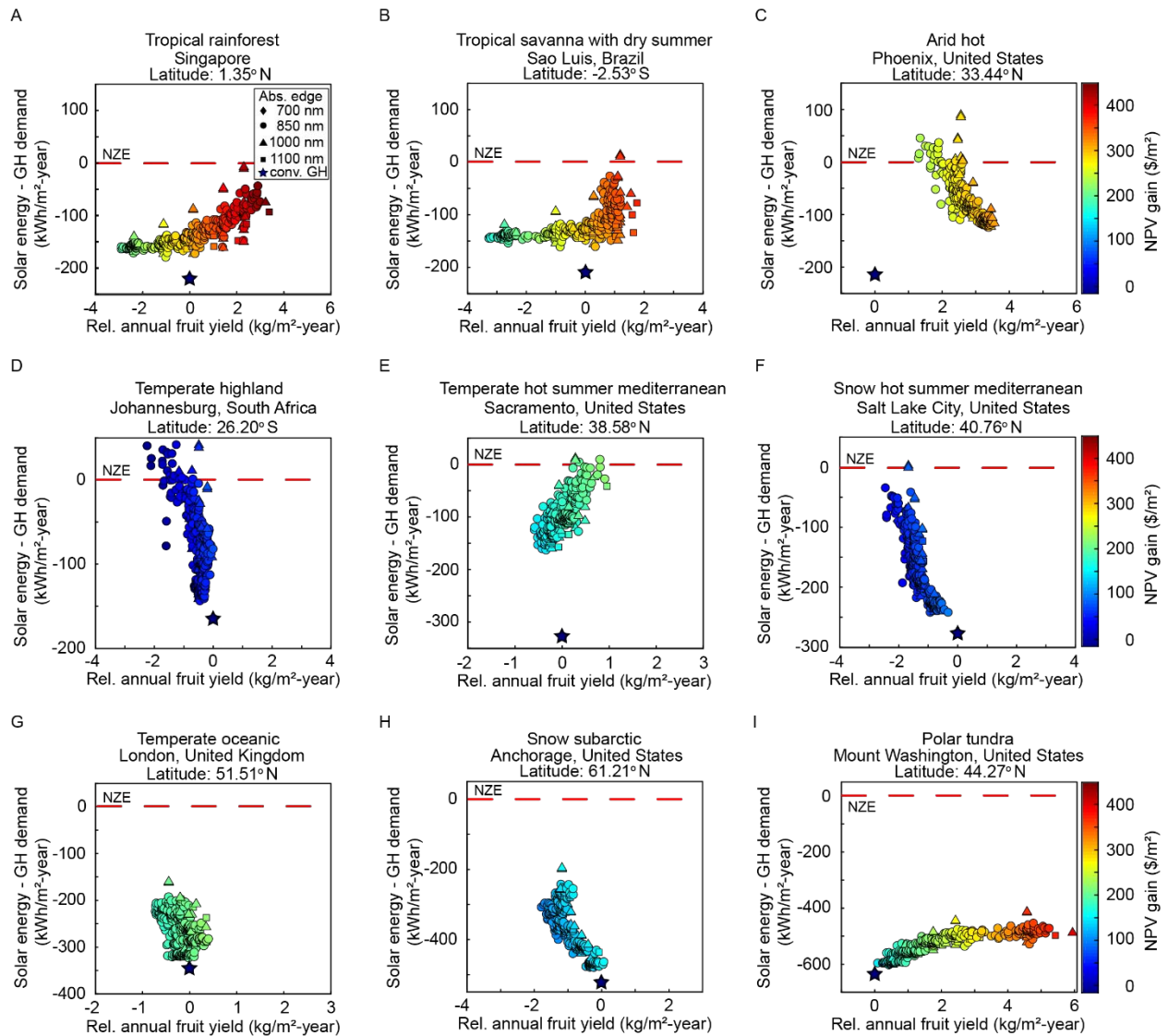


Figure 4. The relative gain in “base case” NPV per unit greenhouse floor area when adding OSCs as a function of relative annual tomato fruit yield and difference between solar energy and greenhouse demand across nine distinct climates. The data includes modeling 64 OSC active layers organized by the cells absorption edge. The specific location modeled for a given climate classification is listed above the plots. Lettuce yield and NPV gain is measured relative to the conventional greenhouse system for each climate. The performance of the conventional system is given by a star symbol for each climate.

3.3 OSC-greenhouse system considerations

Through modelling, we infer that both lettuce and tomato production can benefit from OSC integration onto greenhouses in most climates, with marginal to significant gains in NPV relative to the conventional greenhouse. In considering the performance optimization across climates there are several insights that become apparent. In warm climates close to the equator, integrating the OSCs onto the greenhouse structure can improve crop production in both lettuce and tomato. These climates experience both high ambient temperatures and greater insolation than climates found at higher latitudes. As a result, the conventional greenhouses require the use of shade cloths throughout the year to limit overheating and potential light induced plant stress.²¹ In the OSC-greenhouses, the solar cells provide thermal management benefits by reducing transmittance into the greenhouse space across the visible and near IR, and through the low-emissivity of the ITO electrodes providing improved IR management.²⁴ The improved thermal management reduces the amount of time the greenhouse exceeds its high temperature set-point resulting in positive benefits to plant yield.²³ The growth saturation with radiation is depicted by the variation in annual lettuce yield as a function of average annual DLI for the arid hot climate in **Figure S4(A)**. Here we see that, an average annual DLI of 13-17 moles/m²-year was optimal for lettuce with a higher DLI resulting in drop in yield. In addition, the lower operating temperatures reduce heat stress resulting in improved crop production. This dependence on temperature is exemplified in **Figure S4(A)** where the OSC-greenhouse shows comparable annual lettuce yield to the conventional greenhouses at about 5 % lower average annual DLI due to the better temperature control through IR rejection.

Throughout all the climates considered, we see that in the absence of supplemental lighting, the maximum gain in NPV for OSC greenhouses is obtained through low OSC roof area coverage for high PCE OSCs or high roof area coverage for moderate PCE OSCs with high transmittance over the PAR spectrum. On the other hand, maximum roof area coverage for high PCE OSCs was preferable when supplemental lighting was introduced. Despite considering 64 different OSC active layer blends, we see that the model consistently showed that OSCs with IEICO-4F and Y6 acceptors resulted in the best performance. Both SMAs have absorption that extends into the near IR. When blended with a suitable polymer donor, IEICO-4F based OSCs have PCE demonstrated over 12 % while Y6 base OSCs have PCE of 16 % - 18 %. While IEICO-4F based blends have transmittances of the order of 45 % - 60 % in the PAR wavelength region, Y6 based blends have

a transmittance under 20 %. Hence these two materials demonstrate the flexibility in OSC designs in balancing PCE, PAR transmittance, and OSC roof area coverage.

So far, we limited our discussion to the global economic gains possible in growing lettuce and tomato. However, from an economic point of view, it should be noted that choice of species and cultivar of the plant to be grown in the greenhouse is dependent on local market opportunities, consumer demand and even social conditions. Comparing these lighting needs to other popular greenhouse plants grown worldwide, as shown in **Table S1**, we observe lettuce and tomato to provide reasonable upper and lower light requiring model systems. Hence, while revenues and production cost can change, the relative economic improvements should be broadly applicable.

3.4 Global economic outlook

Scaling back and considering the global opportunities to improve the economic outlook of greenhouses while also offsetting energy demand through the integration of OSCs, we map the optimized system performances across the globe based on climate classification. The maximum gain in NPV of the OSC-greenhouse compared to a conventional greenhouse for growing lettuce in each climate is given in **Figure 5(A)**. Whereas in **Figure 5(B)** we broadly categorize climates based on the OSC-greenhouse net energy demand and yield irrespective of the systems NPV. We find that greenhouses operating in dry and tropical climates at latitudes lower than 35° show potential for NZE greenhouses with minimal drop in yield. These locations also provide the highest gain in NPV with respect to the conventional greenhouse (\$310/m²). At latitudes between 35° to 40°, temperate, dry and snow climates tend to have a relatively long and cold winters, thereby achieving only a partial energy offset without yield loss. Nevertheless, the addition of OSC to the greenhouse increase the system economic potential with maximum gain in NPV being approximately \$85/m². Snow and polar climates at latitudes higher than 40° are characterized by low solar insolation, long winter and high energy demand leading to a drop in power generation potential while also resulting in a drop in lettuce yield with respect to conventional greenhouses. These locations partially offset greenhouse energy demand but result in a marginal, if any, gain in NPV. Overall, across all 25 simulated climates a maximum NPV of about \$870/m² is seen for lettuce production in OSC-greenhouses.

The maximum gain in NPV for an OSC-greenhouse relative to a conventional greenhouse when growing tomato across different climates is mapped in **Figure 6(A)**, while the OSCs' ability

to balance the trade-off between energy offset and yield loss irrespective of NPV for a particular climate is shown in **Figure 6(B)**. In modeling tomato, the use of supplemental lighting limits significant drops in fruit yield but results in an increase challenge in achieving NZE greenhouses. OSC-greenhouses at latitudes lower than 35° were found to achieve tomato production without a drop in fruit yield and achieve net zero energy. These locations provide a high gain in NPV that can be up to $\$320/\text{m}^2$ higher than that of conventional greenhouses. At latitudes between $35^\circ - 40^\circ$, temperate, dry and snow climates experience a higher energy demand and while complete energy offset is possible, the drop in solar insolation results in a slight drop in fruit yield, despite the presence of supplemental lighting. However, the addition of the OSCs results in substantial energy savings, while the supplemental lighting ensures there is not a significant drop in fruit yield, leading to a maximum gain in NPV of up to $\$75/\text{m}^2$ with respect to conventional greenhouses. At latitudes higher than 40° , the combination of a long winter coupled with additional supplemental lighting energy demand results in no selected location showing potential to achieve both net zero energy and negligible loss in tomato yield. Contrary to lettuce production in greenhouses, the supplemental lighting protects against significant yield loss while the OSCs produce power and assist in greenhouse thermal management through their low emissivity character provided by the ITO electrodes. Hence a positive NPV gain is still seen in all the subgroups within the temperate and snow climate. Polar climates provide a similar outlook to snow climates with the simulated location showing a high gain in NPV leading to about $\$390/\text{m}^2$ increase with respect to conventional greenhouses (**Figure 4(I)**). While these locations are likely unsuited for greenhouse production, the addition of the OSCs does improve their economic outlook.

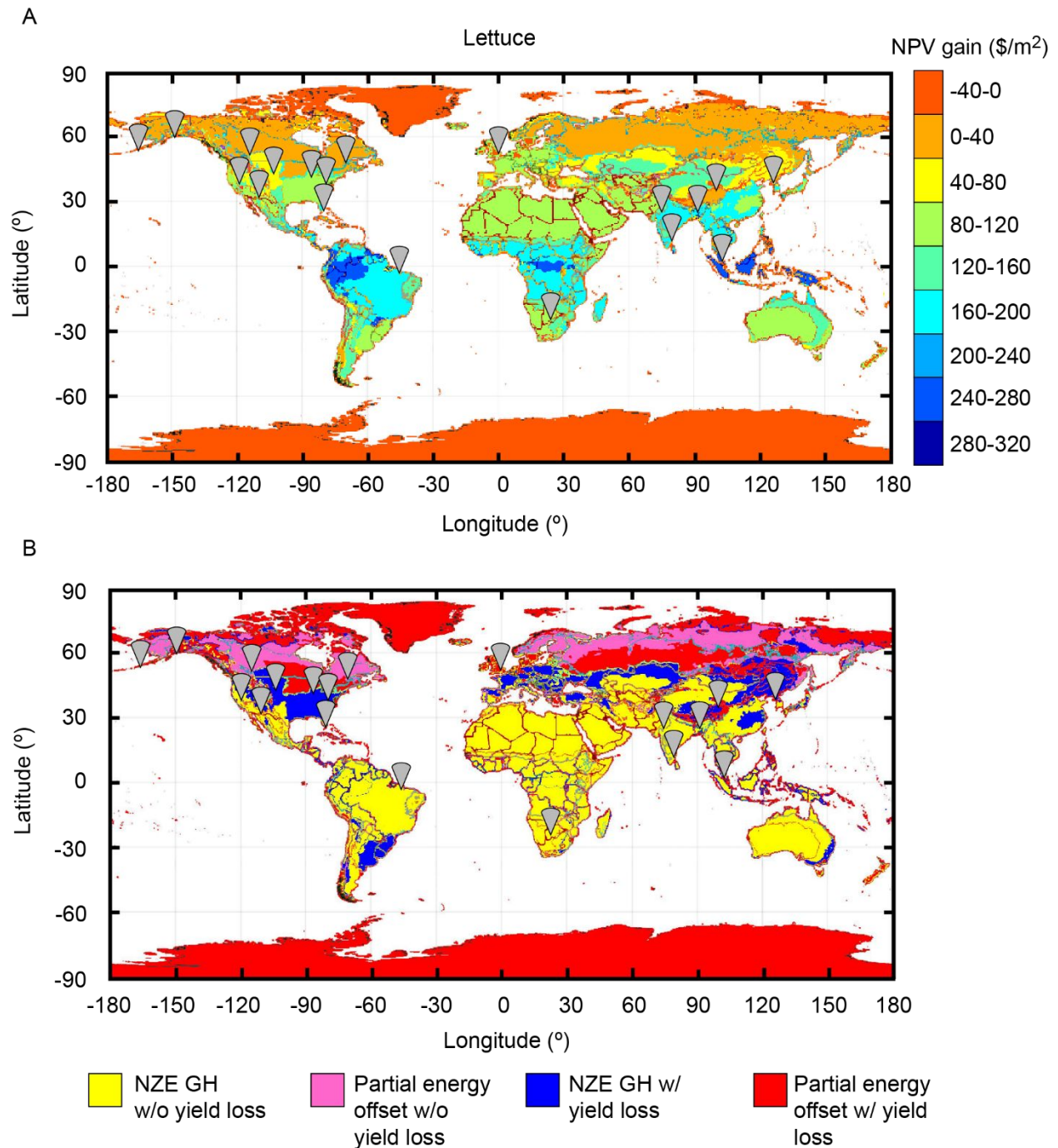


Figure 5. World map that highlights (A) maximum NPV value for ST-OSC greenhouse relative to a conventional greenhouse operating in different climates classified based on the Köppen-Geiger classification system, (B) tradeoffs between power generation and annual lettuce yield in a ST-OSC greenhouse. Indications in the figure depict broadly the simulated locations in this work.

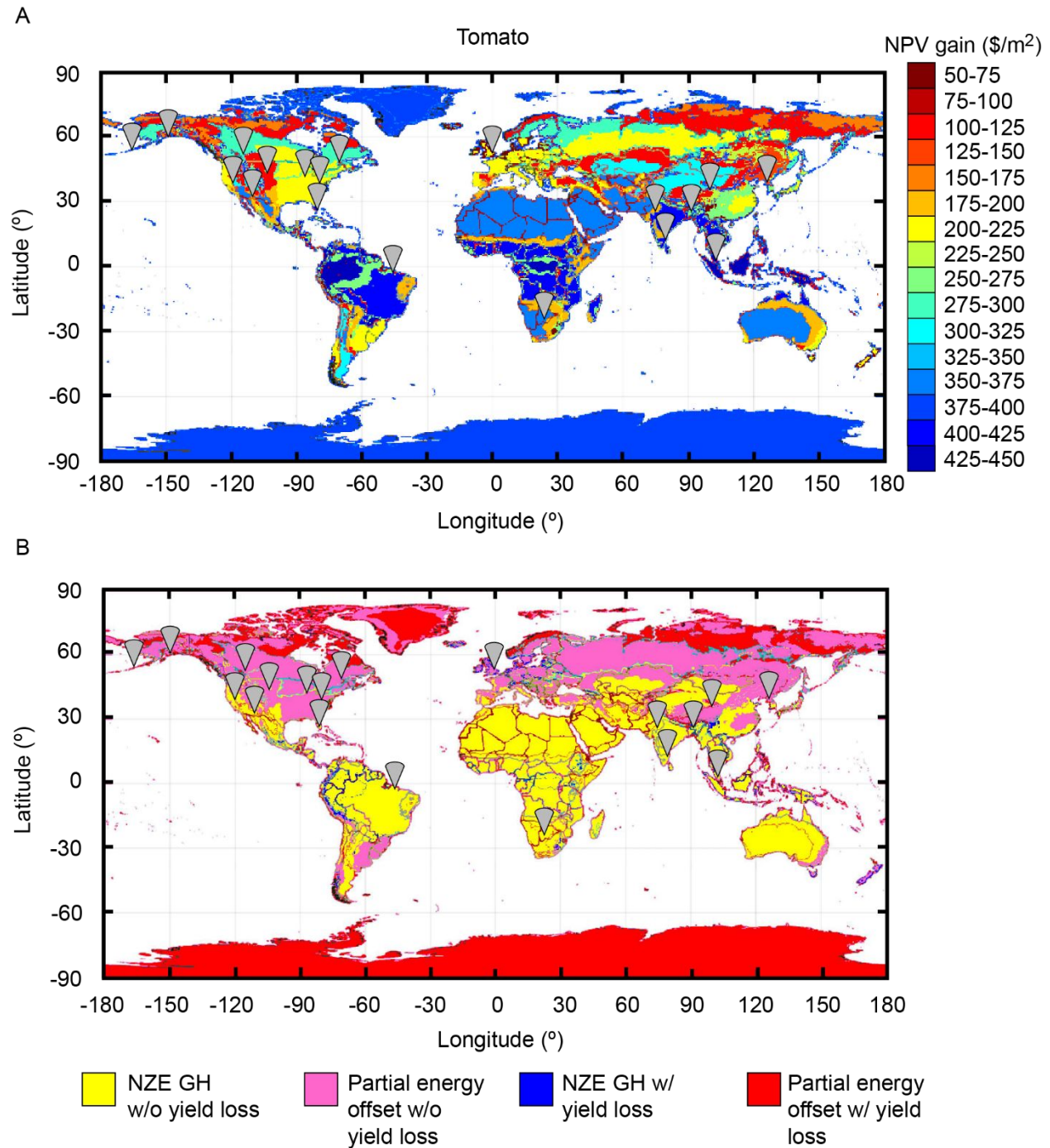


Figure 6. World map that highlights (A) maximum NPV value for ST-OSC greenhouse relative to a conventional greenhouse operating in different climates classified based on the Köppen-Geiger classification system, (B) tradeoffs between power generation and annual tomato yield in a ST-OSC greenhouse. Indications in the figure depict broadly the simulated locations in this work.

4 Conclusions

With increasing world population, there is a need to scale up food production and ensure local fresh food across seasons in a sustainable manner. A controlled environment such as greenhouses satisfies the requirement to increase food production but consumes significantly higher energy in comparison to conventional farming techniques. Hence, there has been immense interest in integrating solar power in greenhouses, with OSCs providing an opportunity to balance power generation and light transmission for plant growth. Here, we formulated a detailed greenhouse system model that combines a detailed accounting of greenhouse environment (temperature, humidity, lighting) with a functional plant growth model, solar power generation from OSCs, and system economics. Through this holistic model, we can assess the economic opportunity of adding OSCs to greenhouses. We focused on modelling two greenhouse crops, lettuce, and tomato, and performed an OSC-greenhouse system optimization considering 64 different OSCs with various fractions of roof coverage. We also considered 25 distinct climates to gain a perspective of the global opportunity given the climate dependence of system performance. Through this optimization process we find that OSC-greenhouses growing lettuce can achieve net zero energy with negligible (under 5 %) drop in annual yield in 11 of the considered 25 climates. When growing tomato, the model results in a similar finding for 10 of the 25 climates. The modeling also shows that there can be significant increases in NPV of greenhouses when adding the OSCs. We observe NPV is extremely sensitive to changes in plant yield and maximum gains in NPV were observed when the systems operated at the maximum solar power production without significant impact on plant yield. Hence, in the absence of supplemental lighting, the maximum gain in NPV for OSC-greenhouses was obtained through low OSC roof area coverage for high efficiency OSCs or high roof area coverage of moderately efficient but higher transmittance OSCs. With supplemental lighting, the OSCs with lower transmittance and higher PCE were favored. Supplemental lighting proved beneficial in minimizing changes in annual fruit yield while OSCs provided up to a 65 % offset in greenhouse energy demand in cold climates. This results in substantial gains in NPV with respect to the conventional greenhouse. Further experimental research on all aspects of the system from plant growth under OSCs to optimized OSC integration can be guided by this model and provide valuable feedback for further model validation and refinement. Nevertheless, this positive outlook supports and fortifies the need for continued research and development of semitransparent OSCs for greenhouse integration. These results

provide clear support that OSC integration into greenhouses may be part of the solution for a more sustainable agri-food industry.

Acknowledgement

The authors would like to acknowledge the National Science Foundation INFEWS award CBET-1639429 for support of this research.

Author Contributions

E.R. and B.T.O conceptualized the work and analysis of results. E.R. developed the models, performed the investigation, collected the data, and wrote the original draft. R.E.B. contributed to modelling the organic semiconductor optical properties. J.A.H. and J.D. contributed to the economic analysis. B.T.O., H.S., and H.A. supervised the research and contributed to project administration. All authors contributed to editing the paper.

Declaration of Interest

The authors declare no competing interests.

Supporting Information

Supporting information can be found online at <https://doi.org/> (to be completed)

References

- 1 M. Crippa, E. Solazzo, D. Guizzardi, F. Monforti-Ferrario, F. N. Tubiello and A. Leip, *Nat. Food*, 2021, **2**, 198–209.
- 2 G. Bot, N. Van De Braak, H. Challa, S. Hemming, T. Rieswijk, G. V. Straten and I. Verloot, *Acta Hortic.*, 2005, **691**, 501–508.
- 3 G. L. Barbosa, F. D. Almeida Gadelha, N. Kublik, A. Proctor, L. Reichelm, E. Weissinger, G. M. Wohlleb and R. U. Halden, *Int. J. Environ. Res. Public Health*, 2015, **12**, 6879–6891.
- 4 C. S. Allardyce, C. Fankhauser, S. M. Zakeeruddin, M. Grätzel and P. J. Dyson, *Sol. Energy*, 2017, **155**, 517–522.

- 5 C. J. M. Emmott, J. A. Rohr, M. Campoy-Quiles, T. Kirchartz, A. Urbina, N. J. Ekins-Daukes and J. Nelson, *Energy Environ. Sci.*, 2015, **8**, 1317–1328.
- 6 Q. Liu, Y. Jiang, K. Jin, J. Qin, J. Xu, W. Li, J. Xiong, J. Liu, Z. Xiao, K. Sun, S. Yang, X. Zhang and L. Ding, *Sci. Bull.*, 2020, **65**, 272–275.
- 7 Y. Wang, Y. Chang, J. Zhang, G. Lu and Z. Wei, *Chem. Res. Chinese Univ.*, 2020, **36**, 343–350.
- 8 D. Koo, S. Jung, J. Seo, G. Jeong, Y. Choi, J. Lee, S. M. Lee, Y. Cho, M. Jeong, J. Lee, J. Oh, C. Yang and H. Park, *Joule*, 2020, **4**, 1021–1034.
- 9 P. Bi, S. Zhang, Z. Chen, Y. Xu, Y. Cui, T. Zhang, J. Ren, J. Qin, L. Hong, X. Hao and J. Hou, *Joule*, 2021, **5**, 2408–2419.
- 10 A. Armin, W. Li, O. J. Sandberg, Z. Xiao, L. Ding, J. Nelson, D. Neher, K. Vandewal, S. Shoaee, T. Wang, H. Ade, T. Heumüller, C. Brabec and P. Meredith, *Adv. Energy Mater.*, 2021, **11**, 1–42.
- 11 C. Yan, S. Barlow, Z. Wang, H. Yan, A. K. Y. Jen, S. R. Marder and X. Zhan, *Nat. Rev. Mater.*, 2018, **3**, 1–19.
- 12 Y. Cui, H. Yao, J. Zhang, T. Zhang, Y. Wang, L. Hong, K. Xian, B. Xu, S. Zhang, J. Peng, Z. Wei, F. Gao and J. Hou, *Nat. Commun.*, 2019, **10**, 1–8.
- 13 J. Zhao, Y. Li, G. Yang, K. Jiang, H. Lin, H. Ade, W. Ma and H. Yan, *Nat. Energy*, 2020, **2**, 1–7.
- 14 X. Song, N. Gasparini, L. Ye, H. Yao, J. Hou, H. Ade and D. Baran, *ACS Energy Lett.*, 2018, **3**, 669–676.
- 15 Y. Liu, P. Cheng, T. Li, R. Wang, Y. Li, S. Y. Chang, Y. Zhu, H. W. Cheng, K. H. Wei, X. Zhan, B. Sun and Y. Yang, *ACS Nano*, 2019, **13**, 1071–1077.
- 16 Y. Cui, H. Yao, J. Zhang, K. Xian, T. Zhang, L. Hong, Y. Wang, Y. Xu, K. Ma, C. An, C. He, Z. Wei, F. Gao and J. Hou, *Adv. Mater.*, 2020, **32**, 1–7.
- 17 Y. Xiong, R. E. Booth, T. Kim, L. Ye, Y. Liu, Q. Dong, M. Zhang, F. So, Y. Zhu, A. Amassian, B. T. O'Connor and H. Ade, *Sol. RRL*, 2020, **4**, 1–9.
- 18 V. V. Brus, J. Lee, B. R. Luginbuhl, S. J. Ko, G. C. Bazan and T. Q. Nguyen, *Adv. Mater.*, 2019, **31**, 1–26.
- 19 M. Fernández Castro, E. Mazzolini, R. R. Sondergaard, M. Espindola-Rodriguez and J. W. Andreasen, *Phys. Rev. Appl.*, 2020, **14**, 1–13.

- 20 C. Zisis, E. M. Pechlivani, S. Tsimikli, E. Mekeridis, A. Laskarakis and S. Logothetidis, *Mater. Today Proc.*, 2020, **21**, 65–72.
- 21 E. Ravishankar, M. Charles, Y. Xiong, R. Henry, J. Swift, J. Rech, J. Calero, S. Cho, R. E. Booth, T. Kim, A. H. Balzer, Y. Qin, C. Hoi Yi Ho, F. So, N. Stingelin, A. Amassian, C. Saravitz, W. You, H.W. Ade, H. Sederoff and B. T. O'Connor, *Cell Reports Phys. Sci.*, 2021, **2**, 100381-100398.
- 22 W. Song, Y. Liu, B. Fanady, Y. Han, L. Xie, Z. Chen, K. Yu, X. Peng, X. Zhang and Z. Ge, *Nano Energy*, 2021, **86**, 106044-106054.
- 23 R. Waller, M. Kacira, E. Magadley and M. Teitel, 2021, **11**, 1–20.
- 24 E. Ravishankar, R. E. Booth, C. Saravitz, H. Sederoff, H. W. Ade and B. T. O'Connor, *Joule*, 2020, **4**, 490–506.
- 25 W. Fu, P. Li and Y. Wu, *Sci. Hortic.*, 2012, **135**, 45–51.
- 26 L. Kong, Y. Wen, X. Jiao, X. Liu and Z. Xu, *Environ. Exp. Bot.*, 2021, **182**, 104326-104351.
- 27 E. J. Van Henten, *Agric. Syst.*, 1994, **45**, 55-72.
- 28 K.J. Boote, M.R. Rybak, J.M.S. Scholberg and J.W. Jones, *HortScience*, 2012, **47**, 1038-1049.
- 29 Z. S. Ilić and E. Fallik, *Environ. Exp. Bot.*, 2017, **139**, 79–90.
- 30 E. P. Heuvelink, *Tomatoes*, CAB international, Boston, USA., 2018.
- 31 M. C. Peel, B. L. Finlayson and T. A. McMahon, *Hydrol. Earth Syst. Sci.*, 2007, **11**, 1633–1644.
- 32 E. J. Van Henten, *Agric. Syst.*, 1994, **45**, 55–72.
- 33 N. Lu, T. Maruo, M. Johkan, M. Hohjo, S. Tsukagoshi, Y. Ito and Y. Shinohara, *Environ. Control Biol.*, 2012, **50**, 1–11.
- 34 A. A. Thwe, P. Kasemsap, G. Vercambre, F. Gay, J. Phattaralerphong and H. Gautier, *Sci. Hortic.*, 2020, **264**, 109185-109192.
- 35 J. Wang, W. Lu, Y. Tong and Q. Yang, *Front. Plant Sci.*, 2016, **7**, 250-259.
- 36 L. F. M. Marcelis, E. Heuvelink and J. Goudriaan, *Sci. Hortic.*, 1998, **74**, 83-111.
- 37 K. R. Cope, M. C. Snowden and B. Bugbee, *Photochem. Photobiol.*, 2014, **90**, 574-584.
- 38 L. A. A. Pettersson, L. S. Roman and O. Inganäs, *J. Appl. Phys.*, 1999, **86**, 487–496.
- 39 P. Peumans, A. Yakimov and S. R. Forrest, *J. Appl. Phys.*, 2003, **93**, 3693–3723.

- 40 M. Kottek, J. Grieser, C. Beck, B. Rudolf and F. Rubel, *Meteorol. Zeitschrift*, 2006, **15**, 259–263.
- 41 E. Fitz-Rodríguez, C. Kubota, G. A. Giacomelli, M. E. Tignor, S. B. Wilson and M. McMahon, *Comput. Electron. Agric.*, 2010, **70**, 105–116.
- 42 ASHRAE, *HVAC APPLICATIONS*, Atlanta, USA, 2015.
- 43 M. Brechner and A. Both, *Hydroponic lettuce handbook*, Cornell Univ. CEA Progr., Ithaca, USA, 1998.
- 44 J. A. Nelson and B. Bugbee, *PLoS One*, 2014, **9**, 1-10.
- 45 D. A. Demers and A. Gosselin, *Acta Hortic.*, 2002, **580**, 83–88.
- 46 D. Katzin, S. van Mourik, F. Kempkes and E. J. van Henten, *Biosyst. Eng.*, 2020, **194**, 61–81.
- 47 S. Wilcox and W. Marion, *Users manual for TMY3 data sets*, NREL, Golden, USA, 2008.
- 48 M. Sengupta, Y. Xie, A. Lopez, A. Habte, G. Maclaurin and J. Shelby, *Renew. Sustain. Energy Rev.*, 2018, **89**, 51–60.
- 49 C. Gueymard, *Sol. Energy*, 2000, **68**, 285–303.
- 50 Y.Li, X.Huang, K.Ding, H.K.M. Sheriff, L.Ye, H.Liu, C.Z. Li, H.W. Ade and S.R. Forrest, *Nat. Comm.*, 2021, **12**, 1-9.
- 51 J. A. Hollingsworth, E. Ravishankar, B. O’Connor, J. X. Johnson and J. F. DeCarolis, *J. Ind. Ecol.*, 2020, **24**, 234–247.
- 52 B. Lee, L. Lahann, Y. Li and S. R. Forrest, *Sustain. Energy Fuels*, 2020, **4**, 5765–5772.
- 53 M. Dorais, *Canadian Greenhouse Conference*, 2003, **9**, 1-9.